cosmetics

MDPI

Article

Kraft Nanolignin as a Multifunctional Bio-Based Ingredient in Cosmetic O/W Emulsions: Stability, Sunscreen and Antioxidant Performance

Nikolaos Bikiaris *, Nikoleta Kioleoglou and Nikolaos Nikolaidis *

Laboratory of Chemistry and Technology of Polymers and Dyes, Department of Chemistry, Aristotle University of Thessaloniki, 54124 Thessaloniki, Greece; nkioleogl@chem.auth.gr
* Correspondence: nikompik@pharm.auth.gr (N.B.); nfnikola@chem.auth.gr (N.N.)

Abstract

In the present work, oil-in-water (O/W) cosmetic emulsions containing nanolignin (NL) at 0.35, 1, and 2% *w*/*w* were developed using a single multifunctional nanoadditive concept, whereby NL simultaneously acts as an antioxidant, rheology modifier, and color/sunscreen booster. Nanolignin was characterized by FTIR, DLS, and SEM, confirming its chemical structure and nanoscale particle size. The emulsions were evaluated in terms of pH and viscosity stability, rheological behavior, colorimetric CIELAB parameters, DPPH radical scavenging activity, and in vitro sun protection factor (SPF). Incorporation of NL led to a slight pH decrease relative to the blank formulation, while maintaining values within the acceptable cosmetic range (pH 4–6), and yielded emulsions with excellent pH and viscosity stability over 28 days of storage. Increasing the NL concentration modified the rheological profile and viscosity, as well as the L*, a*, and b* color coordinates, enabling tunable visual appearance and texture. All formulations exhibited high antioxidant capacity; notably, the NL_1% emulsion displayed higher radical scavenging activity than the NL_2% system, underscoring a non-linear structure–property relationship. SPF values ranged between 14.09 ± 0.875 and 22.29 ± 1.719, demonstrating that nanolignin can enhance photoprotective performance. Overall, this study highlights the potential of nanolignin as a single multifunctional nanoadditive for designing stable, antioxidant, and photoprotective cosmetic O/W emulsions with adjustable rheology and color.

Keywords: emulsions; oil-in-water (O/W); nanolignin; UV protection; antioxidant properties; cosmetics

Check for updates

Academic Editor: Enzo Berardesca

Received: 12 May 2026
Revised: 8 June 2026
Accepted: 8 June 2026
Published: 10 June 2026

Copyright: © 2026 by the authors. Licensee MDPI, Basel, Switzerland. This article is an open access article distributed under the terms and conditions of the Creative Commons Attribution (CC BY) license.

1. Introduction

Increasing consumer expectations and stricter regulatory frameworks for effective, sustainable, and skin-compatible cosmetic products have accelerated the investigation of bio-based ingredients for topical use [1]. In this context, oil-in-water (O/W) emulsions are among the most employed systems in cosmetics, owing to their favorable sensory attributes, ease of application, and capacity to deliver lipophilic actives within aqueous formulations suitable for everyday skincare [2]. Concurrently, the shift toward greener formulations has driven interest in lignocellulosic materials, particularly lignin, as multifunctional components with UV-shielding, antioxidant, and stabilizing capabilities [3].

Lignin is a complex, heterogeneous biopolymer composed of phenylpropane units derived primarily from p-coumaryl, coniferyl, and sinapyl alcohols. As the second most abundant biopolymer after cellulose, it is increasingly recognized as a renewable substitute

for conventional synthetic ingredients [4]. The high density and diversity of functional groups within its structure impart a broad spectrum of physicochemical properties and enable its exploitation in multiple application fields. In recent years, increasing attention has been directed to lignin as a multifunctional ingredient for biomedical, biotechnological, and cosmetic uses, particularly as a carrier of active substances in drug delivery, controlled release systems, and tissue regeneration, owing to its low solubility, pH-responsive behavior, and high stability [5,6]. Additionally, lignin exhibits intrinsic antioxidant and UV-screening capacity owing to the presence of free phenolic hydroxyl groups and ortho-methoxy substitution on aromatic rings, whereas chromophoric functionalities are responsible for its absorption in the UV-visible region [7]. Incorporation of lignin as a photoprotective agent in sunscreen and day-care formulations has been reported in numerous publications [8–12], as it not only enhances the overall SPF but also improves the photostability of conventional organic UV filters [13].

Kraft lignin, the most abundant form of technical lignins, is generated in large quantities as a by-product of the kraft pulping process, which is the predominant industrial route for producing wood pulp for paper and packaging [14]. Notably, it displays stronger antioxidant activity than the commonly used synthetic antioxidant butylated hydroxytoluene (BHT), while exhibiting low cytotoxicity toward normal mammalian cells and, at the same time, demonstrating promising bioactivity against cancer cell lines [15]. Recent developments in nanoengineering have facilitated the production of lignin nanoparticles (nanolignin), which offer increased surface area, enhanced dispersion, and adjustable interfacial properties, positioning them as promising candidates for advanced cosmetic actives and functional excipients [16]. In this context, nanolignin (NL) is particularly appealing for cosmetics and cosmeceuticals [17–19] as it originates from renewable lignocellulosic resources, can be processed via environmentally benign routes, and combines intrinsic UV-filtering and radical-scavenging capabilities with potential roles in emulsion stabilization. However, there is still limited information regarding the systematic design, preparation, and characterization of cosmetic O/W emulsions containing nanolignin as a single, multifunctional nanoadditive, especially concerning the interplay between colloidal structure, photoprotective performance, and physicochemical stability.

Therefore, the aim of this study was to investigate the potential of kraft nanolignin as a multifunctional ingredient in O/W emulsions. Although lignin-based nanomaterials have been thoroughly explored as green UV filters, SPF boosters, and Pickering stabilizers in model systems, there is still a lack of systematically formulated cosmetic O/W emulsions using NL as a single, multifunctional active. The novelty of this work lies in developing and thoroughly evaluating, to the best of our knowledge, for the first time, both the physicochemical stability and biological functionality of O/W emulsions incorporating NL as a bio-based nanostructured ingredient. Accordingly, the present study aims to: (i) prepare cosmetic O/W emulsions containing well-dispersed nanolignin, (ii) characterize their physicochemical properties, CIELAB values, storage stability, and microstructure, as well as (iii) assess their SPF-related and antioxidant performance, with particular emphasis on elucidating the structure–property relationships governing the behavior of nanolignin within the emulsion matrix. By addressing these aspects, this work fills a relevant gap in cosmetic formulation research and introduces a bio-based nanotechnology platform for the design of skin-care products aligned with current sustainability and safety-by-design requirements.

2. Materials and Methods

2.1. Materials

Kraft nanolignin (NL) was kindly provided by Creative Nano (Athens, Greece). For the preparation of O/W emulsions, olive oil, shea butter, glycerin, cetearyl alcohol, cetyl alcohol, beeswax, xanthan gum, polysorbate 60 (Tween 60), tri-sodium citrate dihydrate, stearic acid, ethylhexylglycerin, and phenoxyethanol were purchased from the Novita Group (Thessaloniki, Greece). 2,2-Diphenyl-1-pikrylhydrazyl (DPPH) radical and 6-Hydroxy-2,5,7,8-tetramethylchroman-2-carboxylic acid (Trolox) were purchased from the Tokyo Chemical Industry (Tokyo, Japan). All other materials and reagents used in this study were of an analytical grade of purity.

2.2. Preparation of the O/W Emulsions

The preparation of the O/W emulsions was conducted according to a technique described in previous works from our group. In brief, Table 1 summarizes the two phases and the utilized substances for the fabrication of the emulsions. Nanolignin (0.35, 1, and 2% *w*/*w*) was initially dispersed in H_2O and ultrasonicated in four cycles of 1 min sonication at 15 W and 80% amplitude using a UP100H sonicator (Hielscher ultrasonics, Teltow, Germany). The prepared solution was then transferred to an aqueous solution of sodium cholate (V = 6 mL, C = 12 mM), and it was probe sonicated for 2 min at 15 W, followed by a 1 min rest, and trisodium citrate dihydrate was subsequently added to the obtained NL dispersion. Xanthan gum was dissolved in glycerin in a separate beaker at 60 °C, and upon complete dissolution, was transferred to the NL aquatic dispersion at the same temperature. Following the mixing of all aqueous-phase components, an Ultra Turrax® homogenizer (T-18 basic, Janke and Kunkel IKA, Cologne, Germany) with a S18N-19G model stem was employed at a speed of 9000 rpm for 5 min to further enhance the homogeneity of the dispersion. The oil phase was heated separately in a water bath at 60 °C until all the substances were dissolved, and it was added dropwise to the water phase under constant mechanical stirring (600 rpm) using a 2020 RZR (Heidolph, Schwabach, Germany) mechanical stirrer until complete homogenization. The prepared emulsions were left under mechanical stirring (400 rpm) for 20 min. Afterwards, a mixture of phenoxyethanol and ethylhexylglycerin (90/10% *w*/*w*) was added as a preservative at room temperature, and mechanical stirring was continued for 10 min. Regarding the O/W formulations, the water phase and the oil phase of the final emulsions were 75% *w*/*w* and 25% *w*/*w*, respectively. One blank emulsion without the addition of NL was also prepared as a control sample. The final volume/weight ratio of the produced emulsions was 150 mL/200 g. The fabricated formulations were stored in sterilized glass sample jars (250 g) at RT. The overall experimental procedure for the NL emulsions is illustrated in Figure 1.

Table 1. Water and oil phases for the preparation of the NL O/W emulsions.

Water Phase (75%)				
Ingredients	Blank	NL_0.35%	NL_1%	NL_2%
Water (g)	140	139.3	138	136
Glycerin (g)	7	7	7	7
Tri-sodium citrate dihydrate (g)	1	1	1	1
Xanthan gum (g)	2	2	2	2
Nanolignin (g)	-	0.7	2	4

Table 1. *Cont.*

Water Phase (75%)				
Oil Phase (25%)				
Olive oil (g)	22	22	22	22
Cetyl alcohol (g)	4	4	4	4
Cetearyl alcohol (g)	4	4	4	4
Stearic acid (g)	4	4	4	4
Shea butter (g)	4	4	4	4
Beeswax (g)	4	4	4	4
Tween 60 (g)	4	4	4	4
Preservatives				
Mixture of phenoxyethanol/ethylhexylglycerin (90/10%*w*/*w*) (g)	4	4	4	4

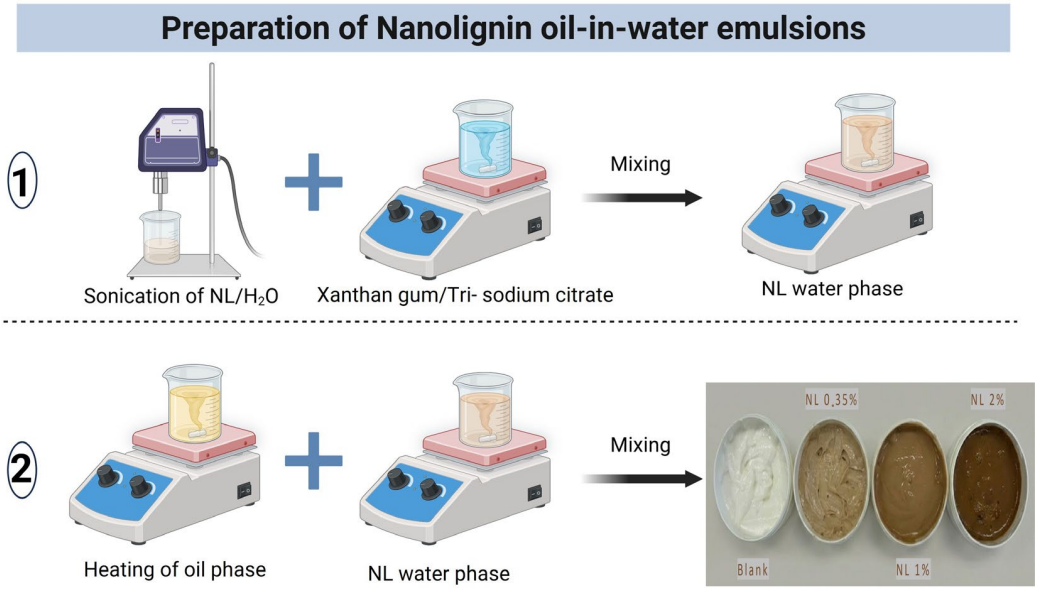


Figure 1. Schematic preparation of nanolignin O/W emulsions. (**1**) NL/H_2O dispersion is sonicated and mixed with xanthan gum and trisodium citrate to form the NL water phase, which is then combined (**2**) with a heated oil phase to obtain emulsions containing 0–2 wt% NL. Created in BioRender. Bikiaris, N. (2026) https://BioRender.com/hr2euz5 (accessed on 22 April 2026).

2.3. pH Measurement

The stability of the prepared emulsions was studied via pH and viscosity measurements after 1, 7, 14, 21, and 28 days of storage at room temperature after the preparation of the emulsion. The pH measurements of the emulsions were read precisely from the instrument by dipping the pH sensor (Microprocessor, WTW, pH 535, Gemini BV, Apeldoorn, The Netherlands), and the mean value of three consecutive measurements (n = 3) was calculated. Variations in the results of pH measurements could not exceed 10% of the initial value for the emulsion to be considered stable.

2.4. Viscosity Determination

Viscosity measurements (n = 3) were performed using the R3 spindle of a Visco Star Plus viscometer (Controla S.A, Thessaloniki, Greece) under 50 and 100 rpm after 1, 7, 14, 21, and 28 days of storage at RT after the fabrication of the emulsions. Apparent viscosity determinations were assessed by dipping the R3 spindle of the viscometer for 1 min in

each of the studied emulsions, and the obtained values were expressed as centipoise (cP). The mean value of three consecutive measurements (n = 3) was calculated. The variation in the results of viscosity measurements could not exceed 10% of the initial value for the emulsion to be considered stable [20].

2.5. Color Measurement

The samples were analyzed at room temperature for color variations using a portable MiniScan XE Plus spectrophotometer (HUNTERLAB, Washington, VA, USA). Color evaluation was conducted by measuring changes in the Commission Internationale de l'Éclairage (CIE) LabCh components. This five-dimensional color space includes L* (lightness), ranging from 0 (black) to 100 (white); a* representing redness (positive values) or greenness (negative values); b* representing yellowness (positive values) or blueness (negative values); and C* (chroma, indicating color saturation) and H* (hue angle) [21].

2.6. Antioxidant Activity (DPPH Method)

The antioxidant activity (AA) of the prepared emulsions was determined via the DPPH (2,2-diphenyl-1-picrylhydrazyl) assay [22]. Specifically, 0.1 g of each sample was dispersed in 10 mL of ethanol (1% w/v) and was added to an ethanol DPPH solution (0.081 mM) in a 1/3 ratio. The reference sample was composed of ethanol and the DPPH/EtOH solution in a 1/3 ratio. The samples were sonicated for 10 min, and their absorbance was recorded after 30, 60, and 90 min of reaction with DPPH in darkness. During the reaction, the DPPH solution color changed from violet to yellow, resulting in a decrease in absorbance, which was measured at 517 nm using a UV-Vis spectrophotometer (UV Probe 1650, Shimadzu, Tokyo, Japan). The free radical scavenging activity was described according to the following equation:

$$\textbf{Free radical scavening activity } (\%) = \frac{\textbf{Absorbance of control} - \textbf{absorbance of sample}}{\textbf{Absorbance of control}} \times \textbf{100} \quad (1)$$

All experiments for each formulation were performed in triplicate for the validation of the obtained results. Results were expressed as mM Trolox equivalent by preparing calibration curves using 0.1 mL methanolic Trolox solutions in the concentration range 0–0.2 mM. The linearity was found up to 0.2 mM concentration of Trolox, and the line was calculated (Figure S1).

2.7. Sun Protection Factor (SPF)

The diluted solution transmittance method was employed for the investigation of the SPF values of the emulsions. Briefly, 1% w/v from each sample was added in ethanol, completely homogenized using sonication, and filtered through Whatman filters. 20% v/v of each solution was diluted with ethanol. The absorption values of the emulsions were achieved in the range of 290–320 nm (every 5 nm) using a UV-Vis spectrophotometer (Shimadzu, Tokyo, Japan). Mansur's equation was utilized to determine the SPF values of the emulsions:

$$\textbf{SPF in vitro} = \textbf{CF} \times \sum_{290}^{320} \textbf{EE}(\lambda) \times \textbf{I}(\lambda) \times \textbf{abs}(\lambda) \quad (2)$$

where CF (correction factor) is 10, EE(λ) is the erythemogenic effect of radiation at wavelength λ, I(λ) denotes the intensity of solar light at wavelength λ, and abs(λ) denotes the absorbance of the sample at wavelength λ. "EE" and × "I" are constants that were first determined in the work of Sayre et al. [23].

2.8. Statistical Analysis

CIELAB color and SPF values were analyzed using Levene's test for verification of homogeneity of variances, followed by one-way ANOVA with Tukey's correction for multiple post hoc comparisons. Data on pH, viscosity, and antioxidant activity were analyzed using repeated measures ANOVA, applying the Greenhouse–Geisser correction to adjust for violations of the sphericity assumption. Post hoc pairwise comparisons were adjusted using the Bonferroni correction, while Tukey's correction was used for multi-group comparisons. All data are presented as mean ± SD, and $p < 0.05$ was considered statistically significant. No normality tests were performed since the number of replicates is three (n = 3), making such tests unreliable and insufficient for assessing distributional assumptions. All analyses were performed using IBM SPSS Statistics v28.0.

3. Results

3.1. Characterization of Nanolignin Particles

To elucidate the chemical structure and main functional groups of the kraft NL, FTIR spectroscopy was employed (Figure 2). The broad band of NL at 3490–3360 cm^{-1} is assigned to the phenolic and aliphatic hydroxyl groups, and the sharper peaks detected at 2935–2840 cm^{-1} are attributed to the C-H stretching vibrations in methyl and methylene groups. The absorbance peak at 1717 cm^{-1} originates from the conjugated carbonyl-carboxyl stretching vibrations, and the sharp peaks located at 1590, 1512, 1463, and 1426 cm^{-1} correspond to the aromatic ring vibrations and C-H deformations. Finally, some characteristic peaks of guaiacyl and syringyl units are detected in the fingerprint region, at 1266, 1143, 857, and 812 cm^{-1}, assigned to the C=O stretching vibration, the C-O stretching vibrations in alcohol groups, the symmetric and asymmetric C–O–C stretching vibrations, the C-H in-plane deformation and out-of-plane vibrations, respectively [24,25].

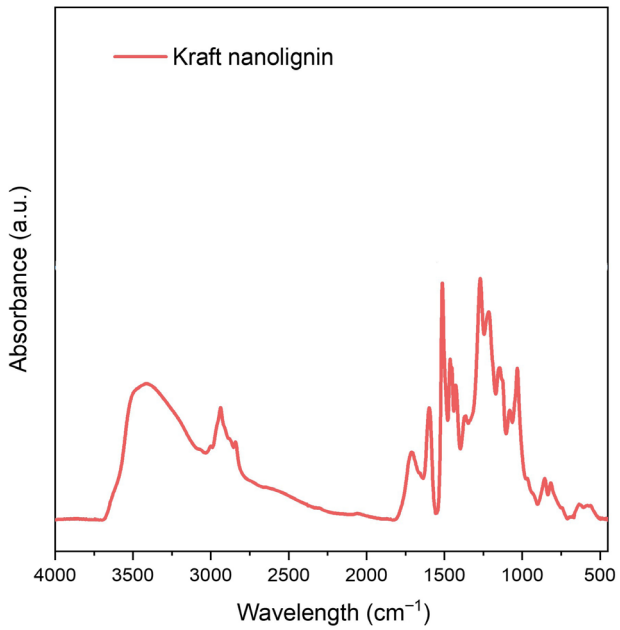


Figure 2. FTIR spectra of pure kraft nanolignin.

Nanolignin exhibited a hydrodynamic diameter (HDD) of 498 nm with a polydispersity index (PDI) of 27% and a moderately narrow distribution, which is supported by the SEM images presented in Figure 3. While the overall morphology remains irregular, the material is organized into compact agglomerates built up from much smaller primary particles. The observed agglomerates typically fall within the ~0.5–2 µm range, and the

primary particles constituting these agglomerates are likely in the submicron size range (approximately 100–500 nm).

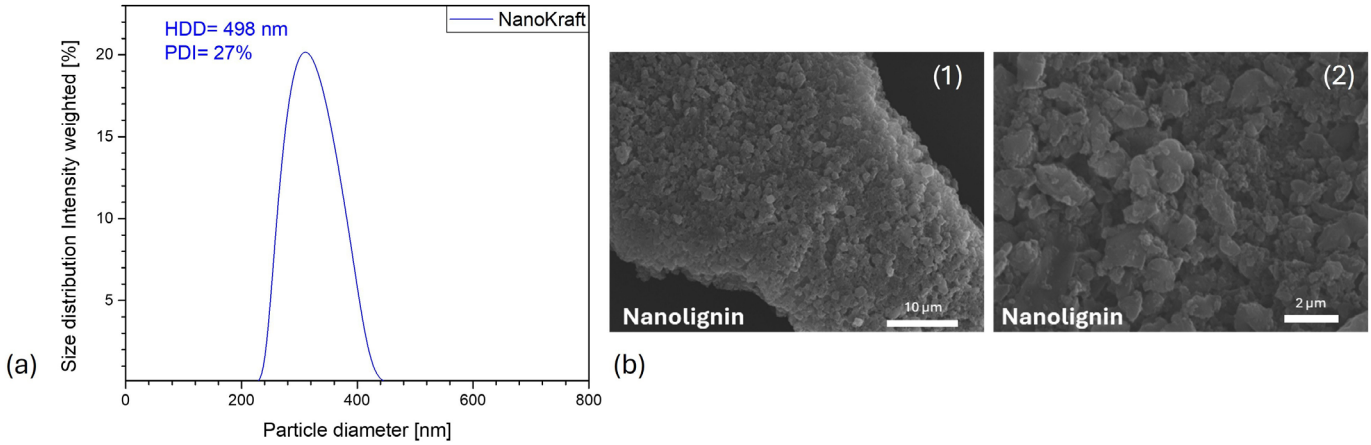


Figure 3. (**a**) Particle size of kraft NL particles measured by DLS and (**b**) SEM images at (**1**) 10 µm and (**2**) µm magnification.

3.2. Stability of the Prepared Emulsions During Storage

The stability of the NL emulsions was evaluated by monitoring their pH and viscosity during storage over a period of 28 days. Throughout this period, all emulsions maintained pH values between 4.5 and 6, which lie within the acceptable range for dermal cosmetic applications (Figure 4). In the blank emulsion, tri-sodium citrate dihydrate helped sustain higher pH values by providing citrate buffering capacity in the aqueous phase, thereby limiting any spontaneous acidification of the formulation [26]. Repeated measures ANOVA analysis did not reveal an effect of emulsion matrix within the group of formulations for all days. Blank emulsion without the addition of NL exhibited higher pH values than the NL-containing emulsions, which showed more acidic pH values, consistent with the presence of ionizable phenolic and carboxylic groups in kraft NL that partially acidify the aqueous phase. This behavior is supported by the FTIR spectrum (Figure 2) of the kraft NL, which reveals characteristic bands of phenolic and carboxylic acid groups. Post hoc pairwise comparisons with Tukey's correction revealed no significant differences in emulsion pH between any of the sampling days, indicating that the formulations were pH-stable over 28 days. This stability can be ascribed to the buffering capacity of the aqueous phase and the relatively low NL ratios used, which did not substantially alter the pH of the continuous phase [27].

The rheological behavior of the prepared emulsions was evaluated over a 28-day period at shear rates of 50 and 100 rpm (Figure 5) and revealed important insights into the flow behavior of the formulation. Only the 100 rpm shear rate exhibited significant effects of time ($p = 0.002$). At 50 rpm, the blank emulsion displays the highest viscosity, starting at 93 P on day 1 and remaining relatively stable through day 28, with a slight mid-storage drop around day 7–14. The addition of NL progressively reduces viscosity in a concentration-dependent manner. The NL_0.35% formulation maintains relatively high viscosity values, not differing from blank ($p > 0.05$), suggesting that at low concentrations, NL does not significantly disrupt the emulsion network. In contrast, NL_1% shows a markedly lower viscosity range, while NL_2% presents the lowest values, indicating that higher NL concentrations interfere with the rheological structure of the emulsion, possibly through the disruption of the surfactant-stabilized interface or the modification of the continuous phase organization. Notably, NL_1% and NL_2% both display the same upward trend toward day 28, which may indicate gradual restructuring or particle network formation over time, potentially reflecting NL aggregation or interactions within

the matrix during storage. At 100 rpm, all formulations exhibit lower absolute viscosity values compared to 50 rpm, which is consistent with the shear-thinning (pseudoplastic) behavior typically observed in cosmetic emulsions. This confirms that the systems are non-Newtonian, where viscosity decreases as shear rate increases. The blank emulsion displayed consistently high viscosity throughout the study, with only a steady increase by day 28, reflecting a lack of structural complexity. Interestingly, this increasing trend is less pronounced or absent in the NL-containing formulations. NL_2% was significantly different from the blank emulsion when examined over the entire timespan ($p < 0.05$). The NL_0.35% formulation presents the highest viscosity among all samples at day 1 (49 cP), but stabilizes from day 7 onward, converging toward the blank values ($p > 0.05$). The NL_1% and NL_2% formulations display the lowest viscosity values throughout the study, further confirming the concentration-dependent viscosity reduction induced by NL.

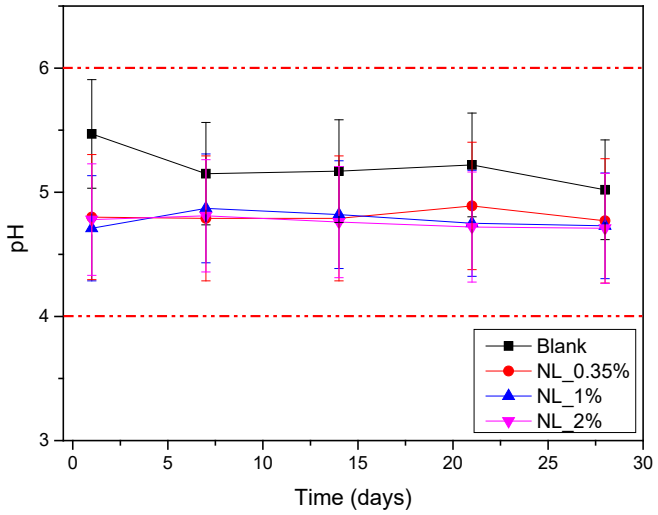


Figure 4. pH values of the NL O/W emulsions during storage stability tests for 28 days.

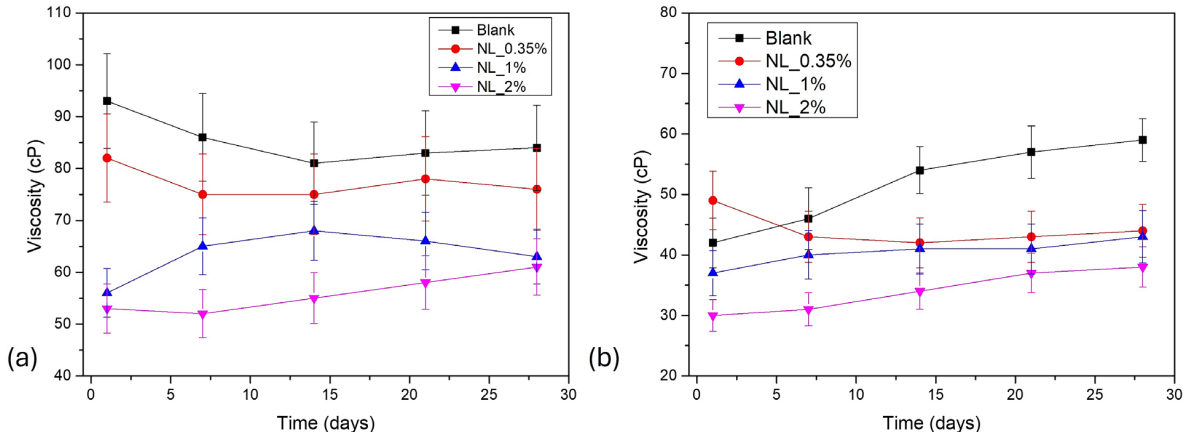


Figure 5. Viscosity values at (**a**) 50 rpm of the prepared emulsions and (**b**) at 100 RPM of the prepared emulsions during 28 days of storage.

3.3. Determination of CIELAB Values

The colorimetric analysis of the creams revealed a significant overall effect on CIELAB values and color strength (L*: $p = 0.002$; a*: $p < 0.001$; b*: $p < 0.001$; C: $p < 0.001$, Table 2). More specifically, the NL_1% and NL_2% emulsions, containing the highest amounts of NL, exhibited the lowest L* value ($p < 0.05$), reflecting decreased lightness, whereas a* values significantly decreased as the amount of NL increased. This suggests that the nanolignin concentration influences the cream's color by decreasing lightness and redness at high

levels. The NL_2% emulsion displayed the lowest a* value of −0.59 ± 1.551 ($p < 0.001$) as well as the highest C value, i.e., 26.56 ± 0.514 ($p < 0.001$), producing a darker brown hue (Figure 6). These results indicate a pronounced shift along the red–green axis, with lower redness and greater color saturation, resulting in a darker brown hue, consistent with the increased presence of NL.

Table 2. CIELAB values obtained from the spectrophotometric color analysis of the emulsions. Mean values within a column with the same letter are not significantly different at $p = 0.05$ using Tukey's post hoc test.

Emulsion	L* (Lightness)	a* (Red–Green)	b* (Yellow Blue)	C (Chroma)	h° (Hue Angle)	R% (Reflectance)	K/S (Color Strength)
Blank	81.90 ± 1.724 ^{ab}	−3.35 ± 0.073 ^{a}	3.31 ± 0.093 ^{a}	4.7 ± 0.100 ^{a}	138.7 ± 5.274 ^{ab}	40.51	0.437
NL_0.35%	78.10 ± 1.622 ^{bc}	−2.61 ± 0.08 ^{b}	8.81 ± 0.235 ^{b}	9.18 ± 0.405 ^{b}	104.1 ± 2.414 ^{bc}	29.18	0.859
NL_1%	75.78 ± 2.027 ^{cd}	−0.78 ± 0.021 ^{c}	16.83 ± 0.419 ^{c}	16.83 ± 0.282 ^{c}	97.23 ± 2.793 ^{cd}	23.86	1.215
NL_2%	71.32 ± 1.551 ^{d}	−0.59 ± 0.025 ^{d}	26.56 ± 0.568 ^{d}	26.56 ± 0.514 ^{d}	89.16 ± 2.583 ^{d}	18.54	2.367

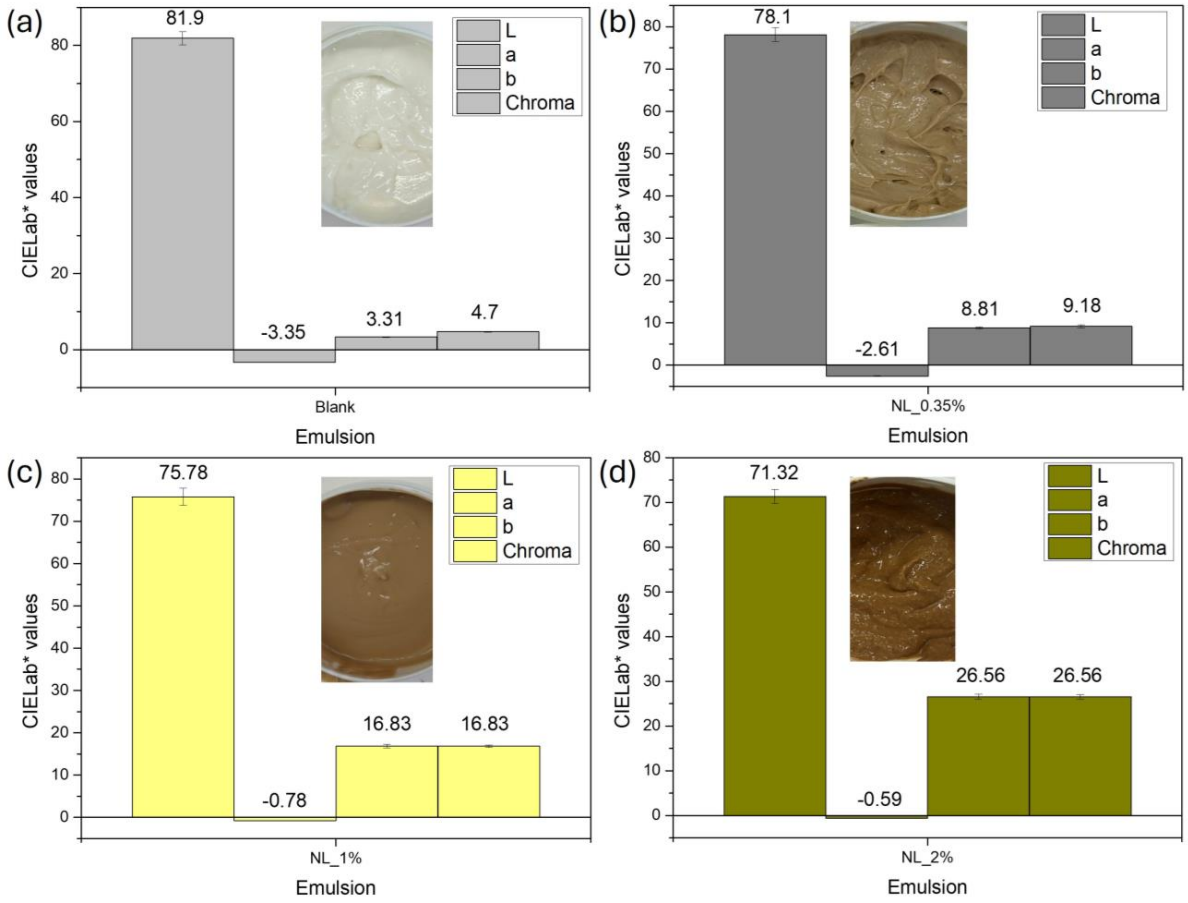


Figure 6. CIELAB color coordinates of (**a**) blank emulsion, (**b**) NL_0.35% emulsion, (**c**) NL-1% emulsion and (**d**) NL_2% emulsion.

3.4. Sunscreen Activity

The quantitative measurement of the effectiveness of a sunscreen is expressed by the sun protection factor (SPF). Figure 7 presents the in vitro SPF values of the emulsions compared to the blank, determined spectrophotometrically to provide a preliminary assessment of their sunscreen efficacy. SPF values were calculated according to Equation (2), and the absorption values were obtained in the range of 290–320 nm. All emulsions exhibited SPF values ranging from 14.09 ± 0.875 to 22.29 ± 1.719, whereas the blank showed a significantly lower value (1.48 ± 0.106; $p < 0.001$), indicating that the incorporation of NL

markedly enhances SPF. NL_2% emulsion presented the highest SPF value (22.29 ± 1.719). Moreover, increasing the NL content from 0.35% and 1% to 2% resulted in a significant increase ($p < 0.001$ and $p = 0.05$, respectively) in SPF. The results demonstrate the capacity of nanolignin to absorb UV radiation, confirming its UV protective potential [28].

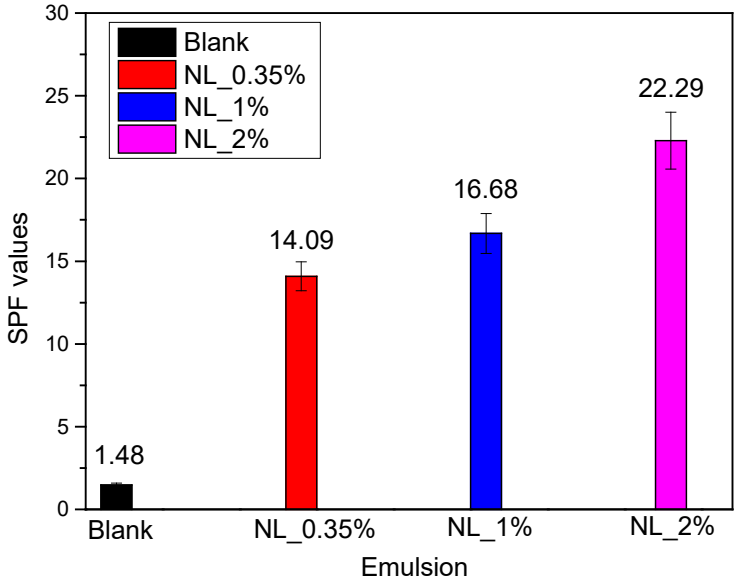


Figure 7. In vitro sun protection factor (SPF) values of the prepared NL emulsions.

3.5. Antioxidant Properties

Antioxidant activity of the creams was assessed over a 90 min period (Figure 8) and expressed as Trolox equivalent antioxidant capacity (TEAC). A significant effect of time and group was detected ($p < 0.001$). All formulations demonstrated time-dependent increase in DPPH scavenging activity, with the most pronounced progression observed in the NL_0.35% emulsion (17.0% at 30 min to 22.5% at 90 min). In addition, the assay revealed substantial antioxidant activity in NL emulsions, with concentration-dependent effects following non-linear kinetics. NL_1% exhibited the highest TEAC value (0.1224 ± 0.013 mM), significantly differing from NL_0.35% ($p < 0.001$) and NL_2% ($p < 0.001$), and achieving 55.6%, 58.1%, and 59.6% DPPH scavenging at 30, 60, and 90 min, respectively. Blank emulsions exhibited the lowest antioxidant activity (2.928% at 90 min) as expected. Despite having the highest amount of nanolignin, NL_2% emulsion displayed moderate antioxidant activity at all time points (Table 3), significantly lower than the NL_1% formulation. This suggests potential aggregation phenomena or steric hindrance effects at elevated NL concentrations, which may reduce the accessibility of the phenolic hydroxyl groups (-OH) responsible for radical scavenging activity [29].

Table 3. Summary of % DPPH scavenging and TEAC (mM TE) for all formulations at 30, 60, and 90 min. Mean values within a column with the same letter are not significantly different at $p = 0.05$ using Tukey's post hoc analysis.

Emulsion	Time					
	30	60	90	30	60	90
	% DPPH Scavenging			TEAC (mM TE)		
Blank	1.085 ± 0.077 ^{a}	1.952 ± 0.132 ^{a}	2.928 ± 0.240 ^{a}	0.012 ± 0.001 ^{a}	0.0137 ±0.001 ^{a}	0.0156 ± 0.001 ^{a}
NL_0.35%	17.89 ± 1.273 ^{b}	20.61 ± 1.431 ^{b}	22.23 ± 1.863 ^{b}	0.044 ± 0.003 ^{b}	0.048 ± 0.005 ^{b}	0.0518 ± 0.004 ^{b}
NL_1%	55.64 ± 3.988 ^{d}	58.13 ± 4.145 ^{d}	59.65 ± 4.678 ^{d}	0.119 ± 0.009 ^{d}	0.119 ± 0.007 ^{d}	0.1224 ± 0.013 ^{d}
NL_2%	43.06 ± 3.071 ^{c}	46.75 ± 3.422 ^{c}	49.24 ± 3.787 ^{c}	0.091 ± 0.007 ^{c}	0.098 ± 0.009 ^{c}	0.1028 ± 0.007 ^{c}

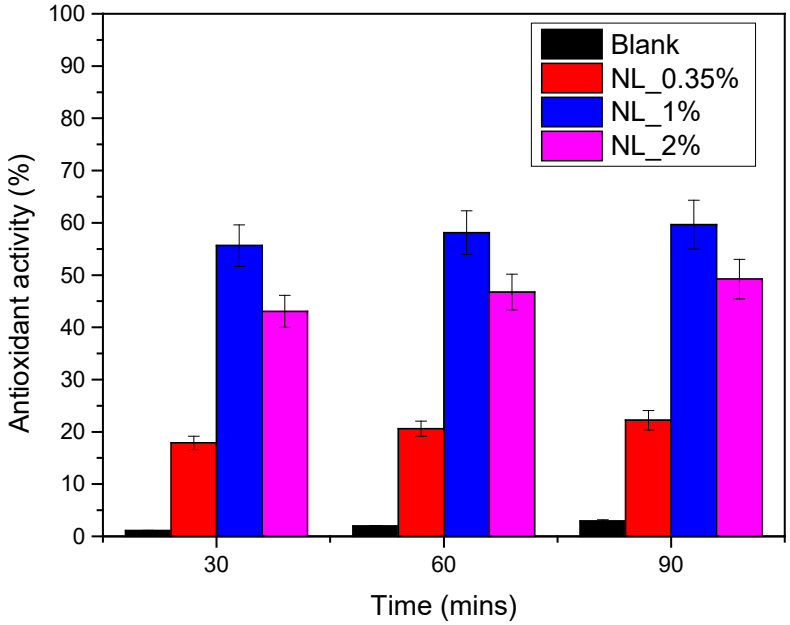


Figure 8. DPPH antioxidant activity (%) of the blank and NL emulsions measured at 30, 60, and 90 min.

4. Discussion

The incorporation of lignin-based nanomaterials in cosmetic formulations represents an emerging frontier in sustainable and green personal care product development [30]. The future use of lignin in cosmetics depends on two main factors: the development of efficient technologies for its modification and the establishment of a stable, economically viable market. In the first case, the self-assembly of lignin into highly ordered nanoparticles can overcome its limited solubility, which currently restricts its application in cosmetic formulations [31]. Recent advances in green chemistry extraction methods already enable the conversion of technical lignin into nanoparticles with controlled size and surface charge accessible for cosmetic applications [32]. Nanoscale processing of lignin enhances the intrinsic antioxidant and UV-protective attributes by improving dispersibility in aqueous emulsion systems, increasing surface area for bioactive interactions, and enabling a more efficient delivery of phenolic antioxidant moieties to target sites [33]. At the same time, market prospects remain positive, with the lignin sector projected to grow at a compound annual rate of about 6% (2020–2026), while demand for lignosulfonates from the pulp and paper industry is expected to increase more modestly, at around 1.6% CAGR [34].

To begin with, it should be noted that the hydrodynamic diameter obtained by DLS (intensity-weighted HDD ≈ 498 nm, Figure 3a) and the SEM observations (agglomerates in the 0.5–2 μm range, Figure 3b) primarily reflect the size of agglomerates in dispersion rather than the size of the primary nanolignin particles. According to the EU Cosmetics Regulation (EC) [35] No 1223/2009 and the European Commission Recommendation 2022/C 229/01 [36], the legal classification as a nanomaterial is based on the number-based size distribution of the constituent particles (1–100 nm) and not on the size of their agglomerates or aggregates. In our work, nanolignin forms micron-sized agglomerates in the aqueous phase but consists of primary particles with at least one dimension in the nanometer range; therefore, it may fall under the regulatory concept of a nanomaterial when used as a cosmetic ingredient. A definitive regulatory classification, however, would require a dedicated number-based particle-size analysis (e.g., TEM-based) performed under the conditions specified in the European Commission Recommendation.

Preserving pH stability in cosmetic emulsions is critical to ensuring product safety, performance, and compatibility with the natural acidic mantle of healthy skin, with an optimal topical range of 4.5 to 6.0. The statistical analysis revealed a significant effect of time on pH, as indicated by the Greenhouse–Geisser corrected p-value of 0.006, and also significant variations ($p < 0.001$) were observed in the tested samples. The minor pH decrease in nanolignin-containing formulations (Figure 4) is attributed to the oxidative breakdown of phenolic compounds inherent in kraft lignin, which release weak organic acids such as formic, acetic, and oxalic acids during storage. Kraft lignin, obtained through the alkaline sulfate pulping process, contains residual sulfur-containing functional groups (thiols, sulfonic acids) and condensed phenolic structures that are particularly susceptible to autoxidation in aqueous environments [37,38]. Importantly, this slight pH reduction remains within the acceptable range for topical cosmetic applications and does not compromise product safety or efficacy.

Spreadability and consumer satisfaction depend strongly on consistent rheological behavior; therefore, viscosity stability is a critical requirement for the usability, shelf life, and overall performance of cosmetic emulsions. The dependence of viscosity on shear rate indicates non-Newtonian flow behavior, which is typical of emulsions and other structured fluids [39]. In particular, the reduction in viscosity at higher shear rates (Figure 5b) is characteristic of shear-thinning (pseudoplastic) systems, where shear disrupts the internal microstructure and thereby facilitates flow. This behavior is advantageous for topical cosmetic creams as it allows easier spreading during application while maintaining stability at rest [40]. The variations in viscosity are closely linked to nanolignin concentration, where higher phenolic content likely contributes to stronger hydrogen-bonding networks and enhanced matrix integrity. Emulsions with higher content of NL, particularly NL_1% and NL_2%, maintained greater rheological consistency and demonstrated optimal structural performance over time, while not yielding any significant variations at 50 and 100 rpm. This may be attributed to nanolignin particles occupying interfacial sites, altering droplet–droplet interactions, or modifying the three-dimensional gel network formed by the emulsifier and thickener system. The overall viscosity stability over 28 days across all formulations indicates that nanolignin incorporation does not compromise the physical stability of the emulsion system, which is a promising finding for its potential use as a functional cosmetic ingredient.

The main techniques used to evaluate lignin color are the Munsell system and the CIELAB method [41]. In cosmetic formulations, color measurements are particularly important, as they provide an objective, quantifiable description of product color that is directly related to consumer perception and acceptance. The characteristic brown to black coloration of lignin-based sunscreens generally limits their inclusion in the widely preferred white, daily use formulations, while potentially making them a more appealing option for individuals with darker skin tones. Herein, CIELAB values of the emulsions revealed that a higher amount of NL results in increased color saturation and lower lightness. This suggests that the increased NL content contributes to stronger pigmentation, likely due to substantially higher density of phenolic chromophoric structures, including quinones, methoxy-substituted phenoxy groups, conjugated carbonyl groups, and aromatic rings (guaiacyl and syringyl units) with conjugated double bonds consistent with the FTIR spectra (Figure 2). These unsaturated functional groups absorb visible light and impart the characteristic brownish color to lignin-based formulations [28]. The inherently dark color of lignin, largely arising from harsh physical and chemical processing conditions (such as elevated temperatures and oxidative modifications), limits its acceptance in cosmetic applications [42]. Nevertheless, darker emulsions are often associated with a higher content

of bioactive compounds, which may enhance their therapeutic efficacy and support the objectives of cosmeceutical formulations.

Exposure to UV radiation (190–400 nm) is the main cause of the generation of radical, reactive oxygen and nitrogen-centered species and related oxidative stress, having a destructive effect on skin health [43]. Radicals are responsible for lipid peroxidation and degradation of elastin and collagen, promoting both loss of skin elasticity and aging [44]. In addition, they react with DNA, promoting apoptosis, genetic mutation, and cancer. An effective sunscreen should absorb broadly between 290 and 400 nm to protect the skin from sunburn and other UV-induced damage [45]. Thus, sun protection constitutes a significant feature of cosmetic products. Using lignin as a UV-blocking ingredient in cosmetic formulations is particularly attractive, as it can enhance both the SPF of cosmetic formulations and increase the photostability of conventional UV filters. The presence of different chromophores and auxochromic groups gives lignin a broad absorption profile across the UV region [46]. Spectrophotometric SPF values (Figure 7) of the studied emulsions revealed that the presence of nanolignin imparts significant sunscreen activity compared to the blank formulation. Furthermore, the results showed that increasing the NL content leads to a significant increase in SPF values. Overall, this preliminary assessment confirmed the UV protective potential of nanolignin.

Radical reactive oxygen species (ROS) contribute to a range of degenerative processes, such as aging and UV-induced inflammation [47], which explains why antioxidants are commonly incorporated into sunscreen formulations [48]. Nanolignin exhibits notable antioxidant properties owing to its phenolic pharmacophore, capable of scavenging ROS and forming highly stabilized mesomeric structures. This was further verified in the current work by the DPPH assay (Table 3 and Figure 8), where it was observed that the addition of NL significantly enhanced ($p = 1$) the antioxidant capacity of the emulsions compared to the blank formulation. In addition, the statistical analysis revealed a significant effect of time on antioxidant capacity, as indicated by the Greenhouse–Geisser corrected value ($p < 0.001$). Notably, the DPPH inhibition achieved by NL_1% is comparable to or exceeds the antioxidant performance reported for cosmetic emulsions enriched with Vitamin C, which reached 30.38 $\pm$ 1.68% DPPH scavenging under similar assay conditions, underscoring nanolignin as a competitive natural antioxidant for topical formulations [49]. All NL-containing formulations exhibited a time-dependent increase in DPPH scavenging activity over the 90 min observation period. This kinetic behavior suggests that higher nanolignin concentrations provide sufficient excess antioxidant capacity to rapidly quench available DPPH radicals, whereas lower concentrations require extended reaction times to achieve maximum scavenging. Regarding the DPPH radical scavenging mechanism, lignin involves both hydrogen atom transfer (HAT) and single electron transfer (SET) pathways, facilitated by the aromatic hydroxyl groups and methoxy substituents within the lignin macromolecular structure [50]. Nanoscale particle formation enhances these reactions by increasing the surface-to-volume ratio and improving dispersion stability compared to bulk lignin materials. The demonstrated antioxidant activity of nanolignin emulsions supports their development as active cosmetic ingredients for multiple product categories, including anti-aging serums, moisturizers, and protective formulations. Finally, the 1% NL concentration, exhibiting the highest TEAC (0.1224 $\pm$ 0.013), represents a practical loading level that balances efficacy with cost-effectiveness and formulation stability.

Future studies will incorporate a detailed characterization of emulsion droplet size and zeta potential, accelerated stability testing, and microbiological preservation efficacy testing (ISO 11930) in order to more fully substantiate the long-term physicochemical and microbiological robustness of the nanolignin formulations.

Lastly, despite the promising functional performance demonstrated in vitro, it is critical to emphasize that the safe implementation of nanolignin in commercial cosmetic products requires comprehensive in vivo dermatological assessment. Specific studies addressing potential skin irritation, sensitization, penetration kinetics through the stratum corneum, and long-term bioaccumulation effects are essential to establish safety profiles that meet regulatory requirements in major cosmetic markets, including the European Union (Cosmetics Regulation EC 1223/2009) and the United States (FDA guidelines). Furthermore, the nanoscale dimensions of these particles necessitate specialized toxicological evaluation protocols that account for size-dependent biological interactions distinct from bulk lignin materials. Only through rigorous in vivo validation can the full potential of nanolignin as a safe, effective, and sustainable cosmetic active ingredient be realized.

5. Conclusions

The advantage of nanolignin as an active ingredient lies in its proven antioxidant and UV-shielding properties, emerging from the reduction on the molecular scale as a consequence of specific non-covalent interactions. In the current preliminary study, O/W emulsions containing 0.35, 1, and 2% *w*/*w* nanolignin ratios were prepared and extensively investigated, to the best of our knowledge, for the first time. Stability tests indicated great viscosity and pH stability for all ratios up to 28 days of storage at room temperature. The emulsions exhibited sufficient sunscreen protection (SPF 22.29 $\pm$ 1.72) at a low NL content of 2%, indicating that complex combinations of synthetic organic and inorganic UV filters may not be necessary. The DPPH assay further verified that the incorporation of NL in the emulsions retains its excellent antioxidant capacity even at low concentrations, which are associated with the existence of bioactive polyphenols in the NL structure. NL_1% yielded 59.65 $\pm$ 4.678% and 0.1224 $\pm$ 0.013, while NL_2% yielded 49.24 $\pm$ 3.787% and 0.1028 $\pm$ 0.007 DPPH scavenging activity and mM TE, respectively. Taken together, these results highlight nanolignin as one of the main alternatives for petroleum-based compounds in cosmetic formulations. Integrating these experiments into subsequent investigations will substantially reinforce the safety and efficacy dossier, yielding a more exhaustive and scientifically robust validation of the proposed formulations.

Supplementary Materials: The following supporting information can be downloaded at https://www.mdpi.com/article/10.3390/cosmetics13030149/s1. Figure S1: Calibration curve of Trolox.

Author Contributions: Conceptualization, N.N.; methodology, N.N.; software, N.B.; validation, N.B. and N.N.; formal analysis, N.K.; investigation, N.K. and N.B.; data curation, N.K.; writing—original draft preparation, N.B.; writing—review and editing, N.N.; visualization, N.B. and N.N.; supervision, N.B. and N.N.; project administration, N.N. All authors have read and agreed to the published version of the manuscript.

Funding: This research received no external funding.

Institutional Review Board Statement: Not applicable.

Informed Consent Statement: Not applicable.

Data Availability Statement: The original contributions presented in this study are included in the article/Supplementary Material. Further inquiries can be directed to the corresponding authors.

Conflicts of Interest: The authors declare no conflicts of interest.

Abbreviations

The following abbreviations are used in this manuscript:

NL	Nanolignin
O/W	Oil-in-Water
DPPH	2,2-diphenyl-1-picrylhydrazyl
SPF	Sun Protection Factor
FTIR	Fourier-Transform Infrared Spectroscopy
DLS	Dynamic Light Scattering
ROS	Reactive Oxygen Species
TEAC	Trolox Equivalent Antioxidant Capacity
BHT	Butylated Hydroxytoluene
HAT	Hydrogen Atom Transfer
SET	Single Electron Transfer

References

1. Couceiro, B.; Hameed, H.; Vieira, A.C.; Singh, S.K.; Dua, K.; Veiga, F.; Pires, P.C.; Ferreira, L.; Paiva-Santos, A.C. Promoting health and sustainability: Exploring safer alternatives in cosmetics and regulatory perspectives. *Sustain. Chem. Pharm.* **2025**, *43*, 101901. [CrossRef]
2. Conti, S.; Padovano, L.; Malacarne, M.C.; Caruso, E. Natural Solid Cosmetics: Innovative Water-in-Oil Emulsions. *Cosmetics* **2026**, *13*, 48. [CrossRef]
3. Vasile, C.; Baican, M. Lignins as Promising Renewable Biopolymers and Bioactive Compounds for High-Performance Materials. *Polymers* **2023**, *15*, 3177. [CrossRef]
4. Jiao, H.; Al-Tohamy, R.; Alsharbaty, M.H.M.; Sun, J.; Xiong, M.; Schagerl, M.; Ali, S.S. Harnessing plant lignin for sustainable materials and chemicals: Integrating biosynthesis, structural diversity, and circular bioeconomy perspectives. *Front. Plant Sci.* **2026**, *17*, 1730538. [CrossRef] [PubMed]
5. Stanisz, M.; Klapiszewski, Ł.; Collins, M.; Jesionowski, T. Recent progress in biomedical and biotechnological applications of lignin-based spherical nano- and microstructures: A comprehensive review. *Mater. Today Chem.* **2022**, *26*, 101198. [CrossRef]
6. Chiani, E.; Beaucamp, A.; Hamzeh, Y.; Azadfallah, M.; Thanusha, A.; Collins, M.N. Synthesis and characterization of gelatin/lignin hydrogels as quick release drug carriers for Ribavirin. *Int. J. Biol. Macromol.* **2023**, *224*, 1196–1205. [CrossRef]
7. Widsten, P. Lignin-Based Sunscreens—State-of-the-Art, Prospects and Challenges. *Cosmetics* **2020**, *7*, 85. [CrossRef]
8. Qian, Y.; Qiu, X.; Zhu, S. Sunscreen performance of lignin from different technical resources and their general synergistic effect with synthetic sunscreens. *ACS Sustain. Chem. Eng.* **2016**, *4*, 4029–4035. [CrossRef]
9. Gordobil, O.; Olaizola, P.; Banales, J.M.; Labidi, J. Lignins from agroindustrial by-products as natural ingredients for cosmetics: Chemical structure and in vitro sunscreen and cytotoxic activities. *Molecules* **2020**, *25*, 1131. [CrossRef] [PubMed]
10. Zhang, H.; Liu, X.; Fu, S.; Chen, Y. Fabrication of Light-Colored Lignin Microspheres for Developing Natural Sunscreens with Favorable UV Absorbability and Staining Resistance. *Ind. Eng. Chem. Res.* **2019**, *58*, 13858–13867. [CrossRef]
11. Lee, S.C.; Yoo, E.; Lee, S.H.; Won, K. Preparation and application of light-colored lignin nanoparticles for broad-spectrum sunscreens. *Polymers* **2020**, *12*, 699. [CrossRef] [PubMed]
12. Bikiaris, N.D.; Koumentakou, I.; Lykidou, S.; Nikolaidis, N. Innovative Skin Product O/W Emulsions Containing Lignin, Multiwall Carbon Nanotubes and Graphene Oxide Nanoadditives with Enhanced Sun Protection Factor and UV Stability Properties. *Appl. Nano* **2022**, *3*, 1–15. [CrossRef]
13. Antunes, F.; Mota, I.F.; Fangueiro, J.F.; Lopes, G.; Pintado, M.; Costa, P.S. From sugarcane to skin: Lignin as a multifunctional ingredient for cosmetic application. *Int. J. Biol. Macromol.* **2023**, *234*, 123592. [CrossRef]
14. Argyropoulos, D.D.S.; Crestini, C.; Dahlstrand, C.; Furusjö, E.; Gioia, C.; Jedvert, K.; Henriksson, G.; Hulteberg, C.; Lawoko, M.; Pierrou, C.; et al. Kraft Lignin: A Valuable, Sustainable Resource, Opportunities and Challenges. *ChemSusChem* **2023**, *16*, e202300492. [CrossRef]
15. Widsten, P.; Tamminen, T.; Liitiä, T. Natural Sunscreens Based on Nanoparticles of Modified Kraft Lignin (CatLignin). *ACS Omega* **2020**, *5*, 13438–13446. [CrossRef]
16. Dias, C.; Mersmann, L.; Pires, J.R.; Fernando, A.L. From lignocellulosic biomass to nanolignin: Sustainable solutions for a greener future. *Ind. Crop. Prod.* **2025**, *238*, 122286. [CrossRef]
17. Panariello, L.; Vannozzi, A.; Morganti, P.; Coltelli, M.-B.; Lazzeri, A. Biobased and eco-compatible beauty films coated with chitin nanofibrils, nanolignin and Vitamin E. *Cosmetics* **2021**, *8*, 27. [CrossRef]

18. Rosova, E.; Smirnova, N.; Dresvyanina, E.; Smirnova, V.; Vlasova, E.; Ivan'kova, E.; Sokolova, M.; Maslennikova, T.; Malafeev, K.; Kolbe, K.; et al. Biocomposite materials based on chitosan and lignin: Preparation and characterization. *Cosmetics* **2021**, *8*, 24. [CrossRef]
19. Teno, J.; Pardo-Figuerez, M.; Hummel, N.; Bonin, V.; Fusco, A.; Ricci, C.; Donnarumma, G.; Coltelli, M.-B.; Danti, S.; Lagaron, J.M. Preliminary studies on an innovative bioactive skin soluble beauty mask made by combining electrospinning and dry powder impregnation. *Cosmetics* **2020**, *7*, 96. [CrossRef]
20. Bikiaris, N.D.; Koumentakou, I.; Hatzistamatiou, K.; Lykidou, S.; Barmpalexis, P.; Nikolaidis, N. Preparation and Investigation of the SPF and Antioxidant Properties of O/W and W/O Emulsions Containing Vitamins A, C and E for Cosmetic Applications. *Cosmetics* **2023**, *10*, 76. [CrossRef]
21. Škrlep, M.; Čandek-Potokar, M. Pork color measurement as affected by bloom time and measurement location. *J. Muscle Foods* **2007**, *18*, 78–87. [CrossRef]
22. Baliyan, S.; Mukherjee, R.; Priyadarshini, A.; Vibhuti, A.; Gupta, A.; Pandey, R.P.; Chang, C.-M. Determination of Antioxidants by DPPH Radical Scavenging Activity and Quantitative Phytochemical Analysis of *Ficus religiosa*. *Molecules* **2022**, *27*, 1326. [CrossRef]
23. Sayre, R.M.; Agin, P.P.; LeVee, G.J.; Marlowe, E. A comparison of in vivo and in vitro testing of sunscreening formulas. *Photochem. Photobiol.* **1979**, *29*, 559–566. [CrossRef]
24. Zhou, X.F.; Lu, X.J. Structural characterization of kraft lignin for its green utilization. *Wood Res.* **2014**, *59*, 583–592.
25. Makri, S.P.; Xanthopoulou, E.; Klonos, P.A.; Grigoropoulos, A.; Kyritsis, A.; Tsachouridis, K.; Anastasiou, A.; Deligkiozi, I.; Nikolaidis, N.; Bikiaris, D.N. Effect of Micro- and Nano-Lignin on the Thermal, Mechanical, and Antioxidant Properties of Biobased PLA–Lignin Composite Films. *Polymers* **2022**, *14*, 5274. [CrossRef] [PubMed]
26. Nakamura, K.; Tanaka, T.; Saito, K.; Yokohama, S.; Sonobe, T. Stabilization of minodronic acid in aqueous solution for parenteral formulation. *Int. J. Pharm.* **2001**, *222*, 91–99. [CrossRef] [PubMed]
27. Marquez, R.; Aguado, R.J.; Tarrés, Q.; Tolosa, L.; Tardy, B.L.; Rojas, O.J.; Hubbe, M.A.; Delgado-Aguilar, M. Lignin nanoparticles as Pickering stabilizers: Emulsion engineering through physicochemical design and meta-analysis. *Adv. Colloid Interface Sci.* **2026**, *349*, 103752. [CrossRef] [PubMed]
28. Sadeghifar, H.; Ragauskas, A. Lignin as a UV Light Blocker—A Review. *Polymers* **2020**, *12*, 1134. [CrossRef]
29. Liu, T.; Gao, Z.; Zhong, W.; Fu, F.; Li, G.; Guo, J.; Shan, Y. Preparation, Characterization, and Antioxidant Activity of Nanoemulsions Incorporating Lemon Essential Oil. *Antioxidants* **2022**, *11*, 650. [CrossRef]
30. Evstigneyev, E.I.; Shevchenko, S.M. Structure, chemical reactivity and solubility of lignin: A fresh look. *Wood Sci. Technol.* **2019**, *53*, 7–47. [CrossRef]
31. Mishra, P.K.; Ekielski, A. The self-assembly of lignin and its application in nanoparticle synthesis: A short review. *Nanomaterials* **2019**, *9*, 243. [CrossRef]
32. Yu, H.; Wang, B.; Wang, Y.; Xu, E.; Wang, R.; Wu, S.; Wu, W.; Ji, B.; Feng, X.; Xu, H.; et al. Lignin Nanoparticles with High Phenolic Content as Efficient Antioxidant and Sun-Blocker for Food and Cosmetics. *ACS Sustain. Chem. Eng.* **2023**, *11*, 4082–4092. [CrossRef]
33. Morena, A.G.; Tzanov, T. Antibacterial lignin-based nanoparticles and their use in composite materials. *Nanoscale Adv.* **2022**, *4*, 4447–4469. [CrossRef]
34. Piccinino, D.; Capecchi, E.; Tomaino, E.; Gabellone, S.; Gigli, V.; Avitabile, D.; Saladino, R. Nano-structured lignin as green antioxidant and UV shielding ingredient for sunscreen applications. *Antioxidants* **2021**, *10*, 274. [CrossRef]
35. European Union. Regulation (EC) No 1223/2009 of the European parliament and of the council. *Off. J. Eur. Union L* **2009**, *342*, 59.
36. Rauscher, H.; Kestens, V.; Rasmussen, K.; Linsinger, T.; Stefaniak, E. *Guidance on the Implementation of the Commission Recommendation 2022/C 229/01 on the Definition of Nanomaterial*; Publications Office of the European Union: Luxembourg, 2023.
37. Wang, Y.-Y.; Meng, X.; Pu, Y.; Ragauskas, A.J. Recent advances in the application of functionalized lignin in value-added polymeric materials. *Polymers* **2020**, *12*, 2277. [CrossRef]
38. Espinoza-Acosta, J.L.; Torres-Chávez, P.I.; Carvajal-Millán, E.; Ramírez-Wong, B.; Bello-Pérez, L.A.; Montaño-Leyva, B. Ionic Liquids and Organic Solvents for Recovering Lignin from Lignocellulosic Biomass. *BioResources* **2014**, *9*, 3660–3687. [CrossRef]
39. Ali, A.; Akhtar, N.; Khan, H.M.S. Assessment of physical stability and antioxidant activity of polysiloxane polyalkyl polyether copolymer-based creams. *J. Chem.* **2013**, *2013*, 938042. [CrossRef]
40. Zhai, M.; Zhou, K.; Sun, Z.; Xiong, Z.; Du, Q.; Zhang, Y.; Shi, L.; Hou, J. Rheological characterization and shear viscosity prediction of heavy oil-in-water emulsions. *J. Mol. Liq.* **2023**, *381*, 121782. [CrossRef]
41. Li, C.; Ping, Q.; Shi, H.; Li, N.; Zhang, J.; Wang, C. A rapid and quantitative method for assessing the whiteness of whitened lignin based on an in-depth analysis of reported methods. *Int. J. Biol. Macromol.* **2020**, *156*, 1483–1490. [CrossRef] [PubMed]
42. Wang, J.; Deng, Y.; Qian, Y.; Qiu, X.; Ren, Y.; Yang, D. Reduction of lignin color via one-step UV irradiation. *Green Chem.* **2016**, *18*, 695–699. [CrossRef]
43. Gromkowska-Kępka, K.J.; Puścion-Jakubik, A.; Markiewicz-Żukowska, R.; Socha, K. The impact of ultraviolet radiation on skin photoaging—Review of in vitro studies. *J. Cosmet. Dermatol.* **2021**, *20*, 3427–3431. [CrossRef]

44. Hussen, N.H.A.; Abdulla, S.K.; Ali, N.M.; Ahmed, V.A.; Hasan, A.H.; Qadir, E.E. Role of antioxidants in skin aging and the molecular mechanism of ROS: A comprehensive review. *Asp. Mol. Med.* **2025**, *5*, 100063. [CrossRef]
45. Chen, J.; Liu, Y.; Zhao, Z.; Qiu, J. Oxidative stress in the skin: Impact and related protection. *Int. J. Cosmet. Sci.* **2021**, *43*, 495–509. [CrossRef]
46. Liu, R.; Dai, L.; Xu, C.; Wang, K.; Zheng, C.; Si, C. Lignin-Based Micro- and Nanomaterials and their Composites in Biomedical Applications. *ChemSusChem* **2020**, *13*, 4266–4283. [CrossRef]
47. Sauce, R.; Pinto, C.A.S.d.O.; Velasco, M.V.R.; Rosado, C.; Baby, A.R. Ex vivo penetration analysis and anti-inflammatory efficacy of the association of ferulic acid and UV filters. *Eur. J. Pharm. Sci.* **2021**, *156*, 105578. [CrossRef]
48. Cherubim, D.J.d.L.; Martins, C.V.B.; Fariña, L.O.; Lucca, R.A.d.S.d. Polyphenols as natural antioxidants in cosmetics applications. *J. Cosmet. Dermatol.* **2020**, *19*, 33–37. [CrossRef]
49. Sykuła, A.; Janiak-Włodarczyk, I.; Kapusta, I.T. Formulation and Evaluation of the Antioxidant Activity of an Emulsion Containing a Commercial Green Tea Extract. *Molecules* **2025**, *30*, 197. [CrossRef] [PubMed]
50. Zhao, D.; Zhao, Y.; Yu, L.; Zhao, L.; Yang, M.; Gong, Y.; Mu, S.; Ni, Y.; Peng, L.; Peng, F. Precision-engineered lignin-based antimicrobial and antioxidant nanomaterials: New insights into chemistry, mechanisms, reinforcement strategies and application advances. *Ind. Crop. Prod.* **2026**, *245*, 123295. [CrossRef]

Disclaimer/Publisher's Note: The statements, opinions and data contained in all publications are solely those of the individual author(s) and contributor(s) and not of MDPI and/or the editor(s). MDPI and/or the editor(s) disclaim responsibility for any injury to people or property resulting from any ideas, methods, instructions or products referred to in the content.